INTERNATIONAL SOCIETY FOR
SOIL MECHANICS AND
GEOTECHNICAL ENGINEERING

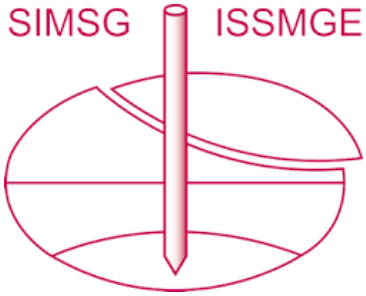

This paper was downloaded from the Online Library of the International Society for Soil Mechanics and Geotechnical Engineering (ISSMGE). The library is available here:

https://www.issmge.org/publications/online-library

This is an open-access database that archives thousands of papers published under the Auspices of the ISSMGE and maintained by the Innovation and Development Committee of ISSMGE.

The paper was published in the proceedings of the 10th International Conference on Physical Modelling in Geotechnics and was edited by Moonkyung Chung, Sung-Ryul Kim, Nam-Ryong Kim, Tae-Hyuk Kwon, Heon-Joon Park, Seong-Bae Jo and Jae-Hyun Kim. The conference was held in Daejeon, South Korea from September 19th to September 23rd 2022.

Physical Modelling in Geotechnics
© 2022 KOREAN GEOTECHNICAL SOCIETY (KGS), Seoul, Korea, ISBN 978-89-952197-7-5

Reduced scale modelling of mechanised tunnelling – challenges and perspectives

G. Viggiani, A.S.N. Alagha & S.K. Haigh
Department of Engineering, University of Cambridge, United Kingdom

ABSTRACT: Mechanised tunnelling causes ground movements that can adversely affect existing structures and services. The cost and complexity associated with field monitoring of tunnelling projects in the urban environment make modelling the advancement of a TBM in a geotechnical centrifuge an attractive proposition. This invited contribution starts with a review of the physical modelling techniques adopted in the past to simulate tunnelling and its impact on existing structures either on the lab floor at single gravity or in a geotechnical centrifuge at increased gravity. In a second part, the paper describes the design and development of a miniature Earth Pressure Balance EPB tunnel boring machine to be used in the Cambridge geotechnical centrifuge and presents some preliminary results of tunnelling in soft clay. Finally, the capabilities and limitations of the proposed mini TBM are discussed together with potential modifications to the current design.

Keywords: Mechanised Tunnelling, Reduced Scale Physical Modelling, Earth Pressure Balance Shield.

1 INTRODUCTION

According to the latest Revision of the World Population Prospects (UN, 2019), by 2050 the world population will be around 9.8 billion, with two-thirds of this living in cities. Increasing urbanisation means growing pressure for supporting infrastructure in cities and towns so that creating underground space may become increasingly relevant to relieve pressure on already densely inhabited areas. In particular, the growing demand for public and sustainable transport has led to a renewed impulse in the construction of urban underground railway lines. Major projects are currently under construction or recently completed all over the world, including Asia (see, *e.g.*, the Jakarta Mass Rapid Rail Transport or the new Delhi Regional Rapid Transit System in India), America (*e.g.,* the Honolulu Rail Transit and Line 3 of Santiago Metro), Australia (*e.g.*, Sydney Metro), and Europe (*e.g.,* the North South Metro Line in Amsterdam, Copenhagen Cityringen, Crossrail - Elizabeth Line in London, Barcelona Metro Line 9, Grand Paris Express, and many others).

The construction of new underground lines and the extension of existing ones require that open excavation and bored tunnelling be carried out in the urban environment, generally in difficult ground, such as soft soils and weak rocks, often below the water table, and almost always in close vicinity of pre-existing structures, such as basements, tunnels, buried pipelines and piled foundations. In this case, the main design requirement is that of limiting tunnelling-induced ground deformations as these may adversely affect the visual appearance and aesthetics of existing structures, their serviceability or function, and, in the most severe cases, their stability.

In the last few decades, the control of tunnelling-induced ground movements has improved significantly due to the considerable advances of mechanised tunnelling technology, with the development of highly specialised Tunnel Boring Machines (TBM) designed to excavate safely and effectively in a variety of ground conditions. In particular, Earth Pressure Balance (EPB) shields are used for operation in soft ground conditions, and are the most commonly adopted type of TBM to tunnel in the urban environment.

Mechanised tunnelling causes complex stress changes at the face of and around the TBM. These produce ground movements that propagate to the ground surface and manifest as a settlement trough above and around the tunnel axis. Although field monitoring of the displacements of the ground and foundations in the proximity of the construction of a new tunnel is possible (*e.g.,* Bakker *et al*., 1999; Selemetas, 2005; Fargnoli *et al*., 2013), the cost and risks associated with field studies make them rare, making modelling the advancement of a TBM in a geotechnical centrifuge an attractive proposition.

The complexity of centrifuge testing and the demands of miniaturisation at increased gravity levels, however, mean that in the past modelling the tunnelling process has generally been highly simplified. In fact, in geotechnical centrifuge studies of tunnelling, excavation has typically been modelled rather crudely using fluid filled flexible tubes in which the volume loss associated to tunnelling can be mimicked by extracting known volumes of fluid, either uniformly along the model tunnel length (*e.g.,* Marshall, 2009) or in stages (Gue, 2017). Only a few examples exist of miniature tunnel boring machines developed to reproduce at least some of

© 2022 KOREAN GEOTECHNICAL SOCIETY (KGS), Seoul, Korea, ISBN 978-89-952197-7-5

the main physical processes taking place during mechanised tunnelling. These have been used either on the lab floor under ordinary gravity (Berthoz *et al*., 2018) or in the centrifuge but, typically, at relatively low *g*-levels (Nomonoto *et al*., 1999).

The development of a miniature TBM capable of excavating in flight at high gravity levels would therefore represent a significant technological breakthrough, enabling realistic simulation of tunnelling-induced soil structure interaction. This paper describes a prototype miniaturised TBM developed at the University of Cambridge to be used in a geotechnical centrifuge at high gravity levels, discusses its potentials and limitations, and presents some preliminary data obtained from tunnelling in soft clay.

2 MECHANISED TUNNELLING

The most common form of Tunnel Boring Machine (TBM) is the Earth Pressure Balance (EPB) shield (Mair, 2008), the main features of which are illustrated in Figure 1. A steel shield, housing the working chamber and the drive motor, terminates with a rotating cutterhead. The permanent lining usually consists of segmental concrete rings assembled and put in place inside the shield by an erector. The cutterhead loosens the soil with blades, cutters and scrapers, and extracts it through openings into the excavation chamber. The opening ratio, defined as the open area in the cutterhead structure divided by the total cutterhead area, varies depending on the soil type. Fine-grained soils do not require much mechanical support at the tunnel face, at least in the short term. Consequently, in most EPB shields, the opening ratio is around 50 – 80% for clays, while a value of 30 – 35 % is usually adopted for sands (Berthoz *et al*., 2018). The bulkhead transfers the pressure of the thrust cylinders to the pliable soil paste. Face support is provided by the excavated material, which is conditioned using foams, slurries, and other additives, to prevent mud caking and soil clogging. The spoil is extracted from the excavation chamber using a screw conveyor (cochlea) which allows regulating the pressure at the face of the TBM. The diameter of the cutterhead is somewhat larger than the diameter of the shield in order to facilitate advancement of the shield and avoid jamming. This overcut should be carefully designed to minimise ground movements as volume losses, and hence ground movements, increase with increasing overcut (Ramoni and Anagnostou, 2011; Cording, 2018). Typical overcut values range between 0.1% and 0.5% of the tunnel diameter. The shield itself is generally telescopic or tapered, with a diameter decreasing by 0.1% to 1% from face to tail, again to avoid jamming and ease steering (Maidl *et al*., 2012). This can cause stress relief and ground movements around the shield body prior to placement of the tunnel lining (Kasper and Meschke, 2006; Ji *et al*., 2008).

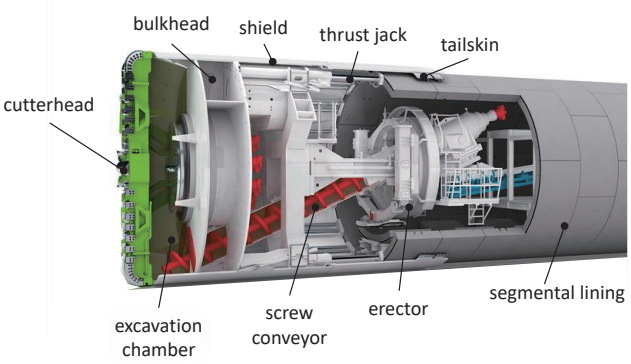

Fig. 1. EPB shield (adapted from Herrenknecht, 2021).

At the rear of shield, a stainless steel wire brush seals the interior working space. The annular gap at the tail of the shield, deriving from the sum of cutterhead overcut, shield tapering, and shield thickness, typically ranging between 120 mm and 180 mm, is one of the most significant sources of volume loss in mechanised tunnelling. In fact, the soil around the excavation boundary will tend to deform and fill the tail gap before ground movements are restrained by the permanent lining.

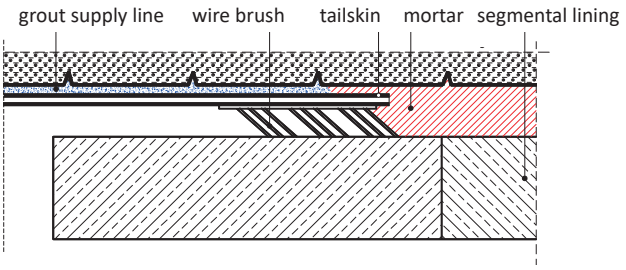

Fig. 2. Tail void grouting (after Thewes and Budach, 2009).

To limit ground movements, it is common practice to fill the gap with a pressurised grouting mortar directly injected through nozzles located in the shield tail, see Figure 2. This technique has widely replaced the practice of grouting through injection holes located in the lining segments, as the latter can only be performed after the erection of the support, thus providing a late and less effective restraint to soil movements around the tunnel. Case histories and experimental data show that movement of the soil at the excavation boundary into this gap can be limited and even eliminated if tail grouting is performed immediately and with adequate pressure.

3 PHYSICAL MODELLING OF TUNNELLING

Reduced scale physical modelling represents a powerful tool to study the main factors affecting ground response to tunnelling. The limited existing field data to assess the effects of tunnelling on existing tunnels are

© 2022 KOREAN GEOTECHNICAL SOCIETY (KGS), Seoul, Korea, ISBN 978-89-952197-7-5

generally obtained in complex environments in which many factors cannot be fully accounted for, nor controlled. Thus, while these data can be useful for the evaluation of design procedures, they have little use to assess parametrically the effect of different factors. In this respect, centrifuge model testing has significant potential, as it can provide controlled testing and boundary conditions.

A variety of modelling techniques have been adopted to model volume loss, ranging from simple trap door tests to sophisticated miniature tunnel boring machines. Starting from the early works of Terzaghi (1936), trap door model tests (Figure 3), have been used to study soil arching above sinkholes in the centrifuge and to estimate loads on buried structures (Vardoulakis *et al*., 1981; da Silva Burke and Elshafie, 2021).

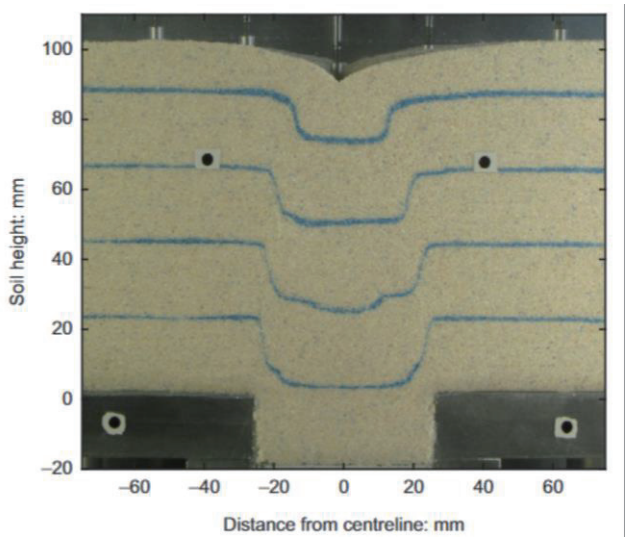

Fig. 3. Observed soil deformation above trapdoor (adapted from da Silva Burke and Elshafie, 2021).

The complexity of centrifuge testing and the demands of increased gravity levels mean that modelling the tunnelling process is generally over-simplified.

A first category of reduced scale model tunnels consists of rigid tubes with flexible faces or rigid movable faces, buried in a centrifuge container. These models have been used mainly to investigate face stability and lining loads for shallow tunnels in sand (see *e.g.,* Chambon *et al*., 1991; Sterpi *et al*., 1996; Kamata and Masimo, 2003). For clay models, the tube has to be inserted sideways after consolidation (Mair, 1979) as the presence of a rigid pipe makes it difficult to consolidate clays in the container.

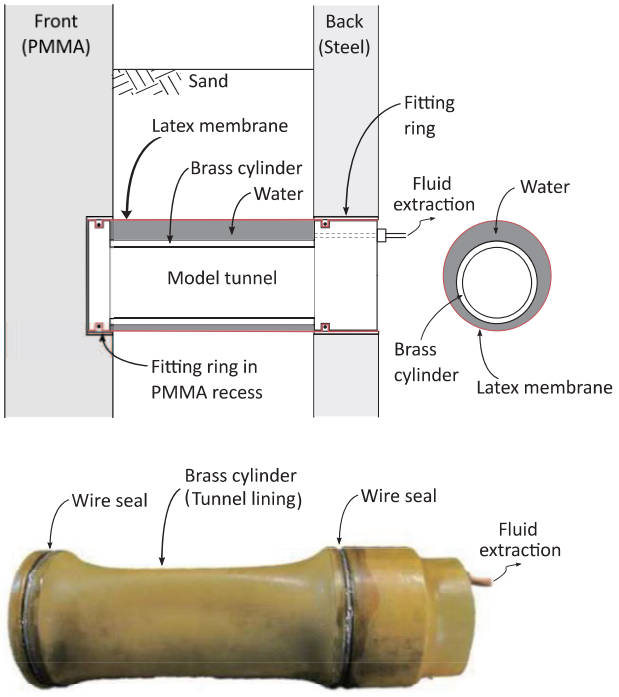

Fig. 4. Experimental set up to simulate tunnelling in a geotechnical centrifuge (after Ritter *et al*., 2018).

The most common model to simulate tunnelling induced volume loss in the centrifuge consists of a thin rubber membrane, inflated with an incompressible fluid and wrapped around a mandrel (Figure 4). During flight, the fluid can be progressively extracted to simulate the effects of volume loss due to tunnelling.

Alternative methods to impose volume loss in similar experimental set-ups have included dissolving polystyrene (Sharma *et al*. 2001), and mechanically reducing the model tunnel diameter (Song and Marshall 2020), in this last case to make it possible to impose non-uniform radial displacements around the tunnel.

Although the simple volume loss models described above have been successfully used to simulate the transverse settlement trough at the end of tunnelling (see amongst others, Atkinson and Potts, 1977; Jacobsz, 2002; Marshall, 2009; etc.), they have common important limitations. The main one being that the tunnelling process is simulated in 2D plane strain conditions, meaning any three-dimensional effects connected to the progressive development of ground displacements in front of an advancing TBM are ignored.

Relatively recently, a number of researchers (*e.g.*, Ng *et al*., 2015; Gue *et al*., 2017; Soomro *et al*., 2018) have adopted a modified system to address this limitation. To obtain realistic longitudinal settlement profiles, in these studies, the model tunnel was divided into independent sections filled with fluid, which could be deflated in sequence through internal drainage pipes to simulate tunnel advancement, see Figure 5. The method is particularly suited to model sequential tunnelling by

© 2022 KOREAN GEOTECHNICAL SOCIETY (KGS), Seoul, Korea, ISBN 978-89-952197-7-5

conventional excavation, such as SCL tunnelling, as the stepped deflation method does not simulate the physical process around the TBM, including the application of a support pressure and a torque at the tunnel face.

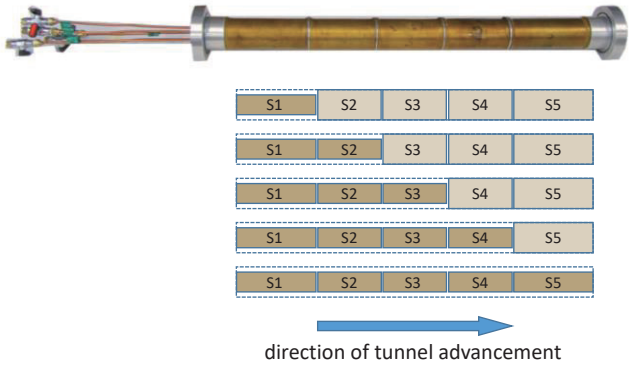

Fig. 5. Sequential deflation tunnelling method (after Gue, 2017).

Mair and Taylor (1997) identified five main sources of ground movements caused by a TBM in the short term, as schematically shown in Figure 6:

1. Stress relief at the tunnel face;
2. Overcutting and shield tapering;
3. Closure of the gap, or tail void, between the back of the shield and the tunnel lining;
4. Lining deflection.

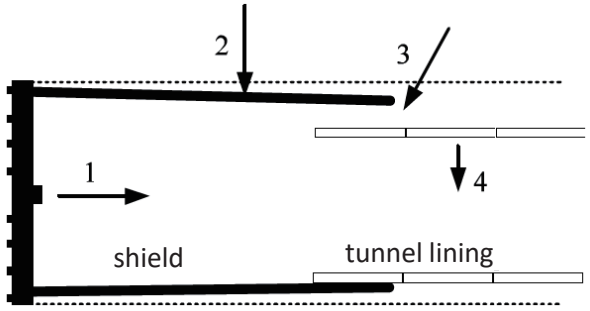

Fig. 6. Sources of volume loss during tunnelling (after Mair and Taylor, 1997).

It is clear that the staged volume loss apparatus is not capable of modelling none of these factors. In fact, other more sophisticated systems exist which allow modelling the gradual process of tunnel excavation in the longitudinal direction in laboratory conditions and account for at least some of the factors above. However, due to their significant size and their cost, to the knowledge of the writers, only seven reduced-scale tunnel boring machines have been developed to date in the world. Six out of seven of these systems were designed to operate under normal gravity, which limits the conclusions, particularly for small scale factors.

Kim *et al*. (2004) presented a small-scale TBM with a 72 mm diameter cutter head, or a scale factor of approximately 1/80. Another miniature TBM was designed and used at Tongji University by Xu *et al*. (2011) with a 400 mm diameter or a scale factor of about 1/15. A significantly larger scale factor was adopted both by the team at the École Nationale des Travaux Publics de l'État (ENTPE), who developed a model TBM with a diameter of 550 mm (Doan, 2007; Berthoz, 2012) and by a team at Southwest Jiaotong University, who used a diameter of 520 mm (Fang *et al*., 2015). In the last case, the geometrical design of the cylindrical shield includes a cutter wheel overcut and a tail void of about 12 mm. Wooden segmental lining is assembled manually inside the shield and the tail void gap injected with hydrated plaster using grouting holes in the model segments, see Figure 7.

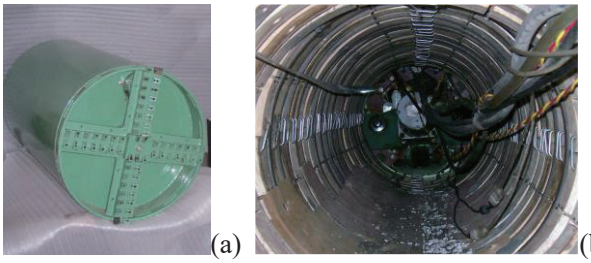

Fig. 7. Southwest Jiaotong University model TBM: (a) front view; (b) arranged segment rings during driving (after Fang *et al*., 2015).

Both these model TBMs are quite large and must advance in sizeable soil chambers, with dimensions of meters, rendering operation of the systems rather cumbersome, as significant amounts of soil must be placed before the test, and removed after the test. More recently, Hu *et al.* (2021) have described systems with an even larger diameter, of 800 mm, to simulate excavation in mixed face condition, including sand and granite, while Liu *et al*. (2022) have described the first reduced scale model of a slurry shield, with a diameter of 500 mm, intended to model tunnelling in cobble soil.

More relevant to this paper, the mini TBM developed by Nomoto *et al*. (1999), with a diameter of 100 mm, is the only one designed for use in a geotechnical centrifuge, see Figure 8. The TBM uses a two-stage process to replicate tunnel construction. First, a shield is driven into dry sand to excavate the tunnel, and then an outer tube is withdrawn to produce a tail void. The model has a diameter of 100 mm and was used to simulate excavation in dry sand under an acceleration of 25*g*, thus modelling a prototype tunnel of 2.5 m diameter.

The machine consists of four primary parts: (i) the 100 mm cutterhead to cut and excavate the soil, behind which there is an excavation chamber to support the tunnel face; (ii) a screw conveyor (coupled with the cutterhead) to extract the excavated soil; (iii) a triple shield tube, the inner tube to host the screw conveyor, the outer tube to act as the shield body and the middle tube, with a diameter 4 mm less than the outer one, and (iv) the drive system, which comprises a cutting motor

© 2022 KOREAN GEOTECHNICAL SOCIETY (KGS), Seoul, Korea, ISBN 978-89-952197-7-5

to run the cutterhead and the screw conveyor, and a thrust motor to push the machine forward and to pull the shield backward.

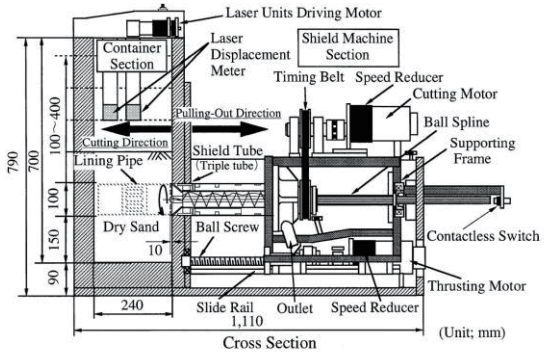

Fig. 8. Experimental setup of the reduced-scale EPB TBM proposed by Nomoto *et al*. (1999).

At the beginning of the test, the shield advances through the soil. After reaching a distance of 230 mm, the outer shield tube is pulled out leaving the smaller diameter middle tube, representing the permanent lining, in place and allowing the creation of a 2 mm tail void gap.

4 NEW MODEL TBM

A model TBM, able to reproduce the mechanisms of shield tunnelling and to account for most sources of volume loss outlined above, has recently been developed at the University of Cambridge, see Figure 9.

The cutterhead has a diameter of 78 mm, while the diameter of the shield at the face is 77.2 mm, giving an overcut ratio of about 1%, which falls within the range of 0.2% and 1.6% reported in the literature (Bezuijen and Talmon, 2008; Ramoni and Anagnostou, 2011; Hasanpour *et al*., 2017; Cording, 2018).

As the proposed mini-TBM was mainly designed to operate in soft clay, a cutterhead with an opening ratio of around 45% was adopted. For the time being, the cutterhead is not equipped with cutting tools, as the current configuration has proven very effective to excavate in soft clay even at high *g*-levels. Potentially, for operation in stiff overconsolidated clay, simple scraping and cutting tools may be attached to loosen the soil and guide it into the working chamber. At the maximum intended acceleration of 50*g* the TBM creates a tunnel diameter equivalent to a prototype of about 4 m.

A conical brass collar is fitted at the front of the lining tube to simulate a tapered shield, with a diameter decreasing from 77.2 mm at the junction with the cutterhead to 76.2 mm at the tail, see Figure 10. The length of the shield is 100 mm, with a length to diameter ratio of 1.3, falling in the range of 1.2 - 3 recommended by ITA (2000) and JSCE (2016). Moreover, the 100 mm length results in a taper gradient of 0.5%, which is in line with the values of 0.1 – 1% reported in the literature (Bezuijen and Talmon, 2008; Ji *et al*., 2008).

The inner diameter of the excavation chamber decreases from 70 mm to 50.8 mm, corresponding to the outer diameter of the inner tube.

The soil is removed from behind the cutterhead by a horizontal auger with a diameter of 40 mm. This is centred by a needle roller bearing at the rear and a bolted connection to the centre of the cutterhead at the front. Three brass rings are welded to the inner brass tube to keep it centred and to support the outer lining tube.

The outer lining tube was carefully chosen to represent extremely stiff lining segments at prototype scale thus eliminating the contribution of lining deflection to the overall volume loss. The front 100 mm of the lining tube were turned down radially by 1.5 mm to allow for the brass collar to slot onto it. The total length of the lining tube is 500 mm, allowing for at least 300 mm of TBM drive.

The auger is driven by a servo motor and a 100:1 reduction drive gearbox that can provide a maximum torque of 27 Nm. The TBM is advanced into a strongbox filled with soil using a linear actuator that can provide a thrust of up to 20 kN.

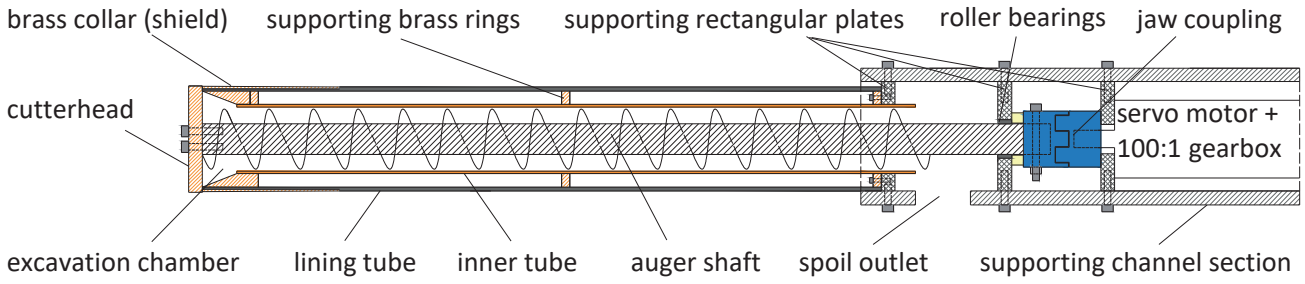

Fig. 9. Conceptual drawing of Cambridge mini TBM.

© 2022 KOREAN GEOTECHNICAL SOCIETY (KGS), Seoul, Korea, ISBN 978-89-952197-7-5

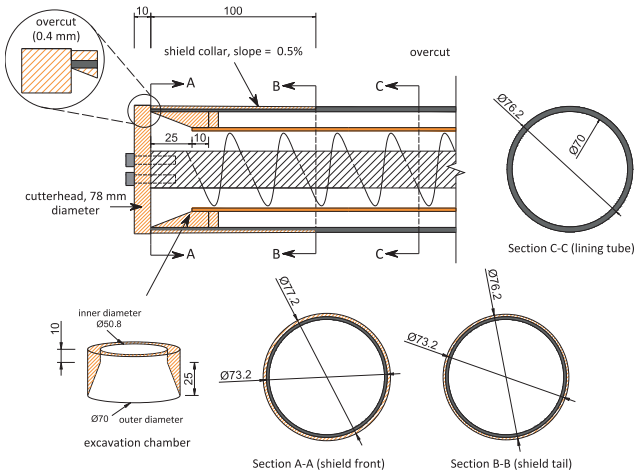

Fig. 10. Geometric details of the cutterhead, shield collar and excavation chamber.

5 OPERATING PARAMETERS

5.1 Auger rotation speed and advance rate

For optimal ground movement control, TBM advance rate and screw rotation speed should be synchronised to maintain the face pressure required for stability. Unlike in real EPB shields, the same horizontal auger serves both the functions of regulating the volume of soil extracted from the excavation chamber and of driving the cutterhead. Nevertheless, the linear actuator and the auger-cutterhead system are controlled independently such that the excavation rate is balanced with the advance rate in order to control the overall volume loss.

Figure 11 is a schematic section through the model shield, defining its dimensions relevant to volume loss calculations, whose values are given in Table 1.

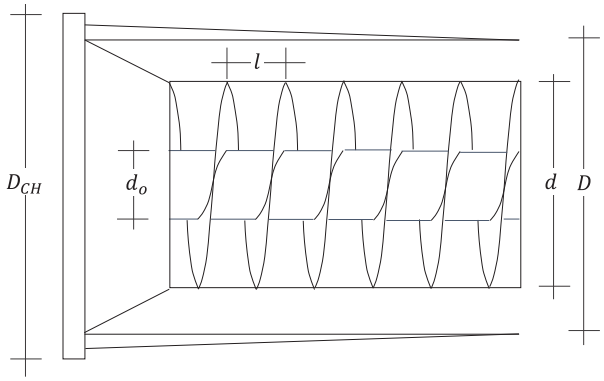

Fig. 11. Schematic section through model TBM.

Table 1. Mini TBM relevant dimensions

D_{CH}(mm)	D (mm)	d(mm)	d_0(mm)	l(mm)
78.0	76.2	46.8	22.2	60.0

The nominal volume of tunnel excavated by the TBM in the time interval Δt is:

$$V = \frac{\pi D^2}{4} v \Delta t \quad (1)$$

where v is the velocity of advancement of the shield.

The volume of soil displaced by the penetration of the model TBM in the same time interval is:

$$V_{\mathrm{d}} = \frac{\pi D_{CH}^2}{4} v \Delta t \quad (2)$$

where D_{CH} is the diameter of the cutterhead. Neglecting the volume of the auger blade, the volume of soil excavated by the auger in the time interval t is:

$$V_{\mathrm{exc}} = \xi \frac{\pi (d^2 - d_0^2)}{4} n l \Delta t \quad (3)$$

where n is the number of revolutions of the auger in the same time interval, ξ is the filling factor of the horizontal auger, d_0 is the diameter of the shaft of the auger, d is the outer diameter of the auger, and l is the pitch of the screw (see Figure 11).

Merritt (2004) and Merritt and Mair (2006) conducted a series of model tests on a horizontal screw conveyor system in soft clay. They concluded that the actual extracted volume corresponds to a filling factor ξ = 65-80% depending on the screw rotation speed and the undrained shear strength of the clay.

The total volume loss can be calculated as the excavated volume in excess of the nominal volume of the tunnel, divided by the nominal volume of the tunnel:

$$V_L = \frac{\mathrm{V_{exc}} - \mathrm{V}}{\mathrm{V}} = \xi \frac{d^2 - d_0^2}{D^2} \frac{nl}{v} - 1 \quad (4)$$

For any target volume loss and for a given advance rate, equation (4) permits to calculate the required auger rotation speed. In particular, to obtain a volume loss of 3% with an advance rate of 14 mm/min, it was necessary to operate the auger at 1.35 rpm. This suggests that the filling factor was slightly higher than suggested by Merritt and Mair (2006), and of the order of ξ = 85%.

Finally, the volume loss around the shield is:

$$V_{LS} = \frac{D_{CH}^2 - D^2}{D^2} = \frac{D_{CH}^2}{D^2} - 1 \quad (5)$$

and the face volume loss is obtained from the total volume loss subtracting the volume loss around the shield:

$$V_{LF} = \xi \frac{d^2 - d_0^2}{D^2} \frac{nl}{v} - \frac{D_{CH}^2}{D^2} \quad (6)$$

5.2 Thrust force and torque

Similar to real shields, the model TBM advances in the soil under the combined action of an axial thrust and a torque, which must be calculated or estimated so that a suitable drive system can be designed.

Based on the data collected for a large number of tunnelling projects, Krause (1987) proposed two very simple empirical relationships to estimate both the required cutterhead torque and thrust force as $T = \alpha D^3$

© 2022 KOREAN GEOTECHNICAL SOCIETY (KGS), Seoul, Korea, ISBN 978-89-952197-7-5

and $F = \beta D^2$, respectively, where D is the diameter of the shield and α and β are two parameters, with dimensions of stress, representing the empirical values for the normal and tangential loads on the unit excavating area and accounting for ground conditions and type and condition of shield.

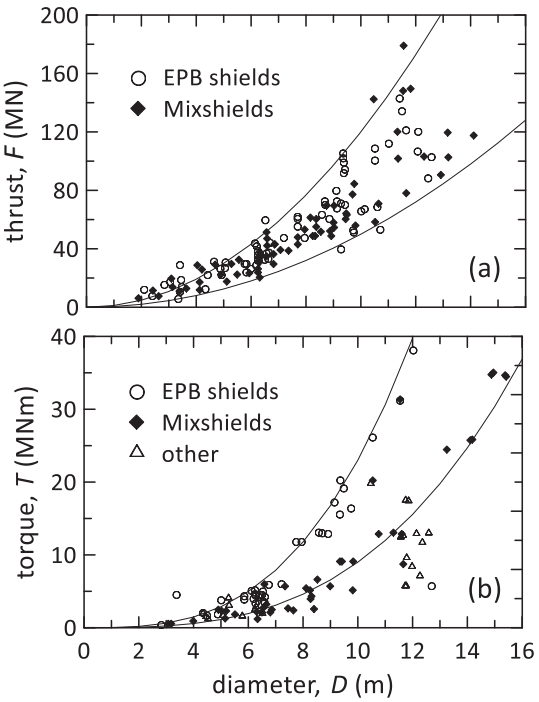

Fig. 12. Operating values of (a) thrust and (b) torque for different shields (modified from Maidl *et al*., 2012).

Figures 12(a) and (b) summarise published values of the operating thrust and torque for various projects around the world, together the empirical relationships by Krause (1987) computed for the ranges of α (= 0.5–1.2 kN/m^2) and β (= 9-23 MN/m^2), determined by the statistical analysis of data gathered for different type of shields. Because parameters α and β have dimensions of stress, they do not scale and can be used directly to estimate the maximum required thrust and torque for the miniature TBM.

Alternatively, the required thrust and torque can be computed considering the interaction between the TBM and the soil during advancement.

As for real shields, the thrust force will have to overcome the total earth pressure normal to the cutterhead surface, proportional to the diameter of the cutterhead squared, the force resulting from the integral of shear stresses on the shield surface, proportional to the average diameter of the shield times its length, and some mechanical losses, due to friction in the sliding rail and in the belt drive of the actuator. Friction develops also at the entrance of the model shield into the box. This is minimised by using a polytetrafluoroethylene (PTFE) ring, and can be estimated by the product of the weight of the mini-TBM by a relevant friction factor

The total jack thrust force of a prototype shield machine may vary slightly during tunnelling but will not directly increase with the tunnelling length. The present version of the mini-TBM, however, does not simulate the installation of the tunnel lining, and the lining tube travels with the shield. Even if the external surface of the lining tube is treated with a lubricant, shear stresses develop at the contact between the lining tube and the clay, so that an increasing thrust is required during tunnel advancement.

Shear stresses developed at the interfaces between the soil and the rotating cutterhead of the model shield, generating resisting torques on the front and the back faces of the cutterhead and on its circumference. The interaction between the auger and the soil in the conveyor also produces a resisting torque that needs accounting for. This can be estimated by computing the work done at the contact between the soil and the inner surface of the conveyor tube and between the soil and the auger flights and ignoring any mechanical torque loss.

6 EXPERIMENTAL RESULTS

Figure 13 shows the layout of a greenfield test carried out using the mini TBM in soft clay, and the position of instrumentation in plan and section.

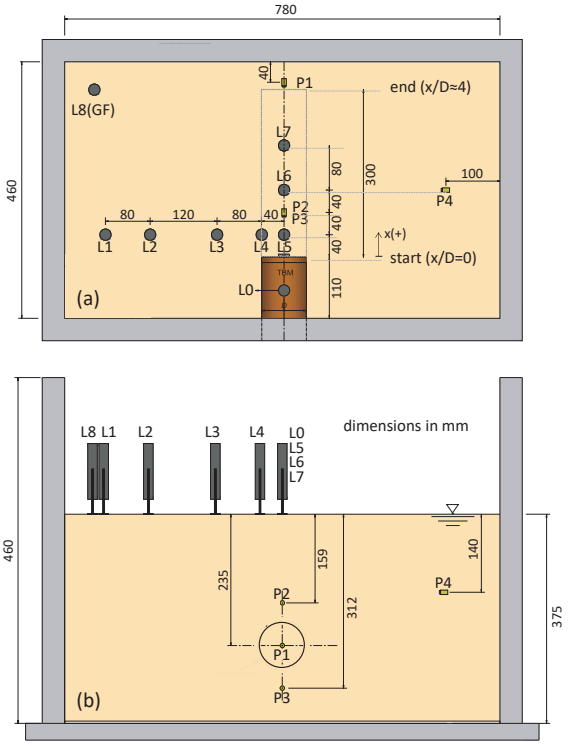

Fig. 13. Layout of instrumentation: (a) plan, (b) section.

The mini TBM started at 110 mm from the front side of the box and advanced by about 300 mm terminating at 50 mm from the end side of the box. The depth of the

© 2022 KOREAN GEOTECHNICAL SOCIETY (KGS), Seoul, Korea, ISBN 978-89-952197-7-5

tunnel axis was 235 mm below the surface of the clay and the water table was at surface. Nine LVDTs (L0 to L8 in Fig. 13) were used to measure surface displacements in the longitudinal and transverse direction and in the greenfield. LVDTs were only placed on one side of the tunnel to permit monitoring of surface displacements on the other side by close-range multi-camera photogrammetry. Because these data have not been processed yet, symmetry was assumed in data reduction. Four pore water pressure transducers (P1 to P4 in Fig. 13) were installed immediately above and below the TBM, in front of its face at the end of the run, and in the greenfield.

Figure 14 compares the measured values of thrust and torque during the advancement of the mini-TBM with the range resulting from the empirical model of Krause (1987) and with the theoretical values computed considering the interaction between the TBM and the soil during advancement.

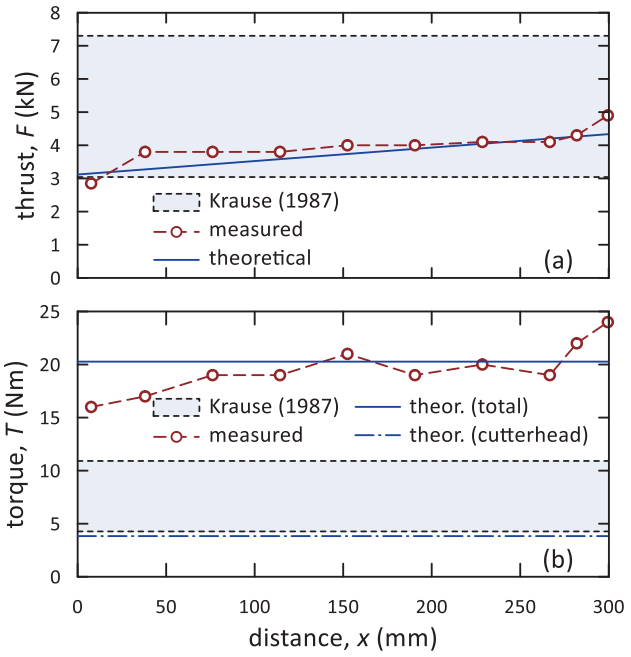

Fig. 14. Operating parameters of mini-TBM: (a) thrust, (b) torque.

The measured thrust falls within the empirical range of Krause (1987). It is relatively small at the start of tunnelling, and then increases to around 4 kN and remains approximately constant during TBM advancement, before increasing sharply at the end of tunnelling. The theoretical model accounts for the friction on the lining and hence predicts that the thrust increases linearly with tunnelling distance. However, to reduce the interaction with the surrounding soil, the lining tube was lubricated, which justifies the roughly constant measured thrust. The small initial value may be connected to the fact that the excavation chamber is initially not fully filled with clay, which reduces the face pressure and hence the required thrust, whereas the sharp increase in thrust towards the end of tunnelling may be attributed to the increased earth pressure on approaching the boundary of the tunnelling box. Imamura *et al*. (1996), Xu *et al*. (2011), and Liu *et al*. (2022) reported similar trends of measured thrust.

The measured torque follows a trend similar to that of the measured thrust, starting from a small initial value, then fluctuating around an approximately constant torque of about 20 Nm, and ultimately increasing sharply towards the end of tunnelling. The initial increase of the required torque is connected to the progressive filling of the auger, which is only complete at an advancement of about 80 mm, whereas the sharp increase at the end of the run may again be attributed to the approaching boundary.

The measured torque agrees very well with the theoretical total torque computed considering the interaction between the TBM and the soil during advancement, but is significantly higher than the empirical range by Krause (1987). This shows the significant role played by the interaction between the auger and the soil in the auger. The theoretical torque computed neglecting this interaction is at the lower bound of the empirical range.

Figure 15 shows the progressive development of the transverse settlement trough with TBM advancement.

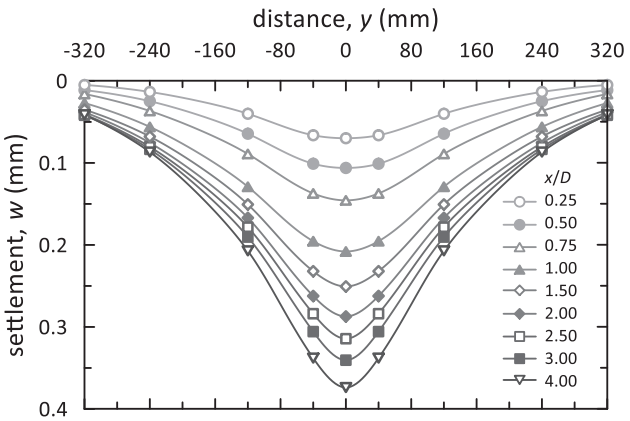

Fig. 15. Transverse settlement trough.

Overall, the transverse settlement profile agrees well with the general pattern found in the literature (Peck, 1969). The settlement trough develops rapidly in the first 150 mm of tunnelling, or $x/D \sim 2$. This distance corresponds to the passage of the tail of the mini-TBM under the monitoring section, indicating that, as expected, the majority of the displacements occurred around the shield. Figure 16 shows the normalised settlement at the positions of LVDTs L1 (at the edge of the settlement trough) to L5 (at the tunnel axis) as a function of the position of the TBM face. The data demonstrate that steady-state conditions were reached at

© 2022 KOREAN GEOTECHNICAL SOCIETY (KGS), Seoul, Korea, ISBN 978-89-952197-7-5

the periphery of the settlement trough but not at the tunnel axis, indicating that the total tunnelling run may have been insufficient.

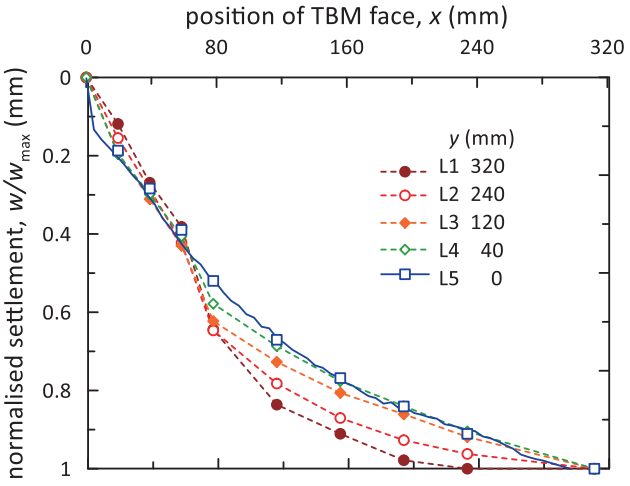

Fig. 16. Longitudinal profile of normalised settlement.

Figure 17 shows the normalised excess pore water pressures measured during and after tunnelling as a function of time, and provides an indication of the position of the mini-TBM at relevant times.

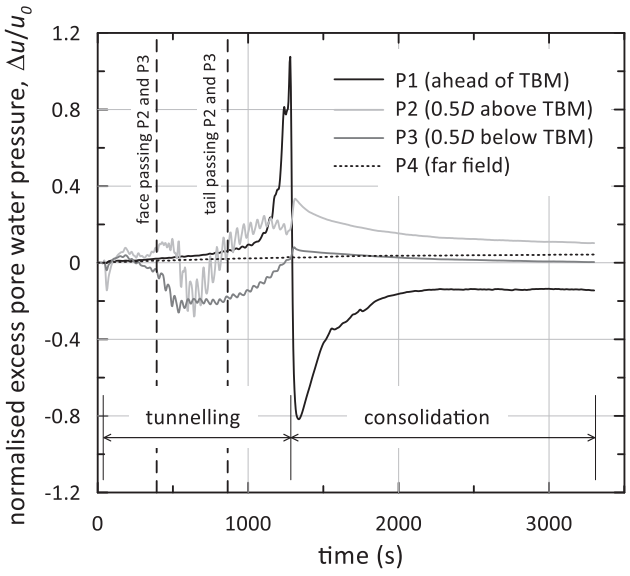

Fig. 17. Normalised excess pore water pressures.

Both pore pressure transducers, P2 and P3, initially recorded suctions due to the stress relief associated to the passage of the model shield body. However, once the tail of the mini-TBM had passed the instrumented section, transducer P2, located half a diameter above the TBM, started recording positive excess pore water pressures, which persisted until the very end of tunnelling. On the other hand, the pore pressures recorded by transducer P3, located half a diameter below the TBM, remained negative and reduced gradually to vanish right at the end of tunnelling. It is interesting that the cycles of the recorded pore water pressure at P2 and P3 are physical as they correspond to the frequency of rotation of the cutterhead. Transducer P1 started measuring large positive excess pore water pressures as the TBM approached the boundary. Immediately after the TBM stopped, these positive excess pore water pressures turned into suctions of almost the same magnitude, indicating that the TBM might have been acting as a plunger. All excess pore water pressures were allowed to dissipate after tunnelling until a steady-state condition was roughly achieved.

7 CONCLUSIONS AND PERSPECTIVE

Several techniques have been used in the past to simulate tunnelling in reduced scale physical models. Plane strain volume loss models have been successfully used in geotechnical centrifuges at high *g*-levels. Although these techniques result in reasonable transverse settlement troughs, they cannot simulate the progressive development of the settlement trough and the interaction between the shield and the soil, which limits the significance of the conclusions when studying tunnel-soil-structure interaction problems. On the other hand, miniature TBMs have been used mostly on the lab floor or at relatively low increased gravity levels, providing only qualitative results because of the unrepresentative stress levels in the model compared to the prototype.

To overcome these limitations, the authors have developed a novel miniature TBM to be used in the Cambridge geotechnical centrifuge at an increased gravity of 50*g*. With a diameter of about 80 mm, the machine is meant to simulate a prototype EPB shield with a diameter of 4 m, and has been used with success to excavate in soft clay. This foundation work has set the basis for further developments and improvements on the current design.

In fact, the total length of tunnelling is currently limited by the sum of the depth of the strong box and the length of the actuator, which are at the limit of what can be hosted on the centrifuge swing. The data presented in Figure 16 indicate that the current length of tunnelling may be insufficient to achieve steady state conditions, particularly in the centre of the surface settlement trough. This is why a second TBM, with a diameter of about 60 mm, is currently under design to be used at an increased gravity of 100*g*, which will result in an increased tunnelling length so as to achieve steady-state conditions in a significant proportion of the model.

Although the current design includes many features of a real EPB shield, such as *e.g.*, the cutterhead overcut, the shield conicity, and the use of a screw conveyor to extract soil from the excavation chamber in a controlled

© 2022 KOREAN GEOTECHNICAL SOCIETY (KGS), Seoul, Korea, ISBN 978-89-952197-7-5

manner to achieve the desired volume loss, some features are less realistically simulated, as there is no tail void gap and the tunnel lining moves with the shield. Neither aspect appears particularly critical. Because the brass collar adopted to model the shield is sotted onto the tube representing the tunnel lining, it can be easily modified to include a tail void gap. As shown by the data in Figure 14, lubrication of the lining tube resulted in minimal shear stress transmission between the lining and the soil during the advancement of the TBM.

Finally, in the current design, the cutterhead is not equipped with cutting tools, because the mini-TBM has only been used to excavate in soft clay. For operation in stiff overconsolidated clay, scraping and cutting tools will be attached to the cutterhead to loosen the soil and guide it into the working chamber. Provision is already been made for tubes running in the space between the inner and outer tube and reaching the excavation chamber, to carry water and/or conditioning fluids to facilitate extraction of the clay from the excavation chamber.

REFERENCES

Atkinson, J.H. and Potts, D.M. 1977. Stability of a shallow circular tunnel in cohesionless soil. *Géotechnique*, 27(2): 203-215.

Bakker K.J., De Boer F., Admiraal J.B.M. and Van Jaarsveld E.P. 1999. Monitoring pilot projects using bored tunnelling: The Second Heinenoord Tunnel and the Botlek Rail Tunnel. *Tunnelling and Underground Space Technology*, 14(2): 121-129.

Berthoz, N., Branque, D., Subrin, D., Wong, H. and Humbert, E. 2012. Face failure in homogeneous and stratified soft ground: Theoretical and experimental approaches on 1g EPBS reduced scale model. *Tunnelling and Underground Space Technology*, 30: 25-37.

Berthoz, N., Branque, D., Wong, H. and Subrin, D. 2018. TBM soft ground interaction: Experimental study on a 1 g reduced-scale EPBS model. *Tunnelling and Underground Space Technology*, 72: 189-209.

Bezuijen, A. and Talmon, A.M. 2008. Processes around a TBM. *Proceedings of the Sixth International Symposium on Geotechnical Aspects of Underground Construction in Soft Ground, IS-Shanghi*, 1-11.

Chambon, P., Corte, J.F. and Garnier, J. 1991. Face stability of shallow tunnels in granular soils. *Proceedings of the International Conference Centrifuge, 99-106.*

Cording, E.J. 2018. *Monitoring and Controlling Ground Behavior at the Source Recent Applications to Pressurized Tunneling*. ITA Muir Wood Lecture 2018.

da Silva Burke, T.S. and Elshafie, M.Z.E.B. 2021. Arching in granular soils: experimental observations of deformation mechanisms. *Géotechnique*, 71(10): 866–878.

Doan, H.V. 2007. *Creusement des tunnels en terrain meuble: étude expérimentale sur modèle réduit de tunnelier à pression de terre en sol cohérent – frottant*. Thèse de doctorat. ENTPE/INSA de Lyon.

Fang, Y., Yang, Z., Cui, G. and He, C. 2015. Prediction of surface settlement process based on model shield tunnel driving test. *Arabian Journal of Geosciences*, 8(10): 7787-7796.

Fargnoli V., Boldini D. and Amorosi A. 2013. TBM tunnelling-induced settlements in coarse-grained soils: The case of the new Milan underground line 5. *Tunnelling and Underground Space Technology*, 38: 336-347.

Gue, C.Y., Wilcock, M.J., Alhaddad, M.M., Elshafie, M.Z.E.B., Soga, K. and Mair, R.J. 2017. Tunnelling close beneath an existing tunnel in clay-perpendicular undercrossing. *Géotechnique*, 67(9): 795–807.

Gue, C.Y. 2017. *Effects of Tunnelling under an Existing Tunnel in Clay*. PhD thesis, University of Cambridge, UK.

Hasanpour R., Schmitt J., Ozcelik Y. and Rostami J. 2017. Examining the effect of adverse geological conditions on jamming of a single shielded TBM in Uluabat tunnel using numerical modeling. *Journal of Rock Mechanics and Geotechnical Engineering*, 9(6): 1112-1122.

Hu, X., Wang, J., Fu, W., Ju, J.W., He, C. and Fang, Y. 2021. Laboratory Test of EPB Shield Tunnelling in Mixed-Face Conditions. *International Journal of Geomechanics*. 21(9): 1-15.

Imamura, S., Nomoto, T., Mito, K., Ueno, K. and Kusakabe, O. 1996. Design and development of underground construction equipment in a centrifuge. *Proceedings of the International Symposium on Geotechnical Aspects of Underground Construction in Soft Ground*, 15-17.

ITA, W. 2000. Mechanized Tunnelling: *Recommendations and Guidelines for Tunnel Boring Machines*. International Tunnelling Association, Lausane, Switzerland.

Jacobsz, S.W. 2002. *The effects of tunnelling on piled foundations*. Ph.D. Thesis. University of Cambridge, UK.

Ji, Q., Huang, Z. and Peng, X. 2008. Analysis on influence of conicity of extra-large diameter mixed shield machine on surface settlement. *Complimentry Special Issue to the Sixth International Symposium on Geotechnical Aspects of Underground Construction in Soft Ground*, 237-242.

JSCE. 2016. *Standard Specifications for Tunnelling-2016: Shield Tunnels*. Japanese Society of Civil Engineers.

Kamata, H. and Mashimo, H. 2003. Centrifuge model test of tunnel face reinforcement by bolting. *Tunnelling and Underground Space Technology*, 18(2-3):205–212.

Kasper, T., and Meschke, G. 2006. On the influence of face pressure, grouting pressure and TBM design in soft ground tunnelling. Tunnelling and Underground Space Technology, 21(2):160-171.

Kim, S.H., Min B.H., Lee, S.H. and You, K.H. 2004. Design and development of tunnelling equipment in a model test. *Proceedings of the 30th ITA-AITES WTC, Singapore*, 19, 4-5.

Krause, T. 1987. *Schildvortrieb mit flüssigkeits-und erdgestützter Ortsbrust*. Mitteilungen des Instituts für Grundbau und Bodenmechanik der Technischen Universität Braunschweig, Heft.

Liu, X., Xiong, F., Zhou, X., Liu, D., Chen, Q., Zhang, J., Han, Y., Xu, B., Deng, Z. and He, C. (2022). Physical model test on the influence of the cutter head opening ratio on slurry shield tunnelling in a cobble layer. *Tunnelling and Underground Space Technology*, 104-264.

Maidl, B., Herrenknecht, M., Maidl, U. and Wehrmeyer, G. 2012. *Mechanised shield tunnelling.* John Wiley & Sons.

Mair, R.J. 1979. *Centrifugal modelling of tunnel construction in soft clay*. PhD thesis, University of Cambridge, UK.

Mair, R.J. and Taylor, R.N. 1997. Bored tunnelling in the urban Environment. *Theme Lecture, Proc. 14th ICSMFE*, *Hamburg*, 2353–85.

Mair, R.J. 2008. Tunnelling and geotechnics: new horizons. *Géotechnique*, 58(9): 695-736.

Marshall, A. 2009. *Tunnelling in sand and its effect on pipelines and piles*. Ph.D. Thesis. University of Cambridge, UK.

© 2022 KOREAN GEOTECHNICAL SOCIETY (KGS), Seoul, Korea, ISBN 978-89-952197-7-5

Merritt, A. S. 2004. *Conditioning of clay soils for tunnelling machine screw conveyors*. Ph.D. Thesis. University of Cambridge, UK.

Merritt, A. N. and Mair, R.J. 2006. Mechanics of tunnelling machine screw conveyors: model tests. *Geotechnique*, 56 (9): 605-615.

Ng, C.W.W., Hong, Y. and Soomro, M.A. 2015. Effects of piggyback twin tunnelling on a pile group: 3D centrifuge tests and numerical modelling. *Géotechnique*, 65 (1): 38-51.

Nomoto, T., Imamura, S., Hagiwara, T., Kusakabe, O. and Fujii, N. 1999. Shield tunnel construction in centrifuge. *J. Geotech. Geoenvironmental Eng. - ASCE*, 125(4): 289-300.

Peck, R.B. 1969. Deep excavations and tunneling in soft ground. *Proc. 7th ICSMFE*, 225-290.

Ramoni, M. and Anagnostou, G. 2011. The interaction between shield, ground and tunnel support in TBM tunnelling through squeezing ground. *Rock Mechanics and Rock Engineering*, 44(1):37-61.

Ritter, S., DeJong, M. J., Giardina, G. and Mair, R.J. 2018. Centrifuge modelling of building response to tunnel excavation. *Int. J. Physical Modelling in Geotechnics*, 18(3): 146-161.

Selemetas D. 2005. *The response of full-scale piles and piled structures to tunnelling*. PhD Thesis. University of Cambridge, UK.

Sharma, J.S., Bolton, M.D., and Boyle, R.E. 2001. A New Technique for Simulation of Tunnel Excavation in a Centrifuge. *Geotechnical Testing Journal*, 24(4): 343-349.

Song, G. and Marshall, A.M. 2020. Centrifuge modelling of tunnelling induced displacements: pressure and displacement control tunnels. *Tunnelling and Underground Space Technology*, 103: 103461.

Soomro, M.A., Ng, C.W.W., Memon, N.A. and Bhanbhro, R. 2018. Lateral behaviour of a pile group due to side-by-side twin tunnelling in dry sand: 3D centrifuge tests and numerical modelling. *Computers and Geotechnics*, 101: 48-64.

Sterpi, D., Cividini, A., Sakurai, S. and Nishitake, S. 1996. Laboratory model tests and numerical analysis of shallow tunnels. *In: Barla, G. (ed.), Proc., Int. Symp. Eurock*, *ISRM, Torino,Vol 1, Balkema, Rotterdam*, 689–696.

Terzaghi, K. 1936. Stress distribution in dry and in saturated sand above a yielding trap-door. *In: Proc. 1st ICSMFE*, 1, 307- 311.

Thewes, M. and Budach, C. 2009. Grouting of the annular gap in shield tunnelling–An important factor for minimisation of settlements and production performance. *Proc. ITA-AITES World Tunnel Congress, Bochum*.

UN (2019). *Revision of World Population Prospects*. UN Department of Economic and Social Affairs: Population Dynamics. https://population.un.org/wpp/ (last accessed, July. 2022).

Vardoulakis, I., Graf, B., and Gudehus, G. 1981. Trap-door problem with dry sand: a statical approach based upon model test kinematics. *Int. J. Numer. Anal. Methods Geomech*, 5: 57-78.

Xu, Q., Zhu, H., Ding, W. and Ge, X. 2011. Laboratory model tests and field investigations of EPB shield machine tunnelling in soft ground in Shanghai. *Tunnelling and Underground Space Technology*, 26 (1):1-14.